Comparison between system design optimization strategies for more electric aircraft network.

Djamel Hadbi, Nicolas Retiere, Frederic Wurtz, Xavier Roboam, Bruno Sareni

Comparison between system design optimization strategies for more electric aircraft network

Djamel Hadbi[a,b,*], Nicolas Retière[a], Frederic Wurtz[a], Xavier Roboam[b] and Bruno Sareni[b]
[a]*University Grenoble Alpes, Grenoble F-38000, France*
[b]*Université de Toulouse, Toulouse 31071, France*

Abstract. The aircraft electric network is a complex system, consisting of many different elements integrated to form a unique entity, designed to perform a well-defined mission. In the current state, the network conceptual design is based on standards defined by the aircraft manufacturer. As a consequence, electric subsystem suppliers are doing local optimizations to fulfill these standards in a separated way through a "mechanistic approach". This results in a set of optimized subsystems which is not necessarily "optimal" with respect to the network level. To overcome this problem, we present a design approach called EPFM (Extended Pareto Front Method) based on separated subsystem optimizations which aims at finding an optimal configuration of the electrical network at the system level. The EPFM is discussed with regard to the computational cost and the collaboration requirements in the aeronautical industrial context and compared with the classical mechanistic approach.

Keywords: System design, integrated optimal design, multilevel optimization, embedded electrical system

1. Introduction

Modern aircraft power systems use the following main forms of energy: mechanical, hydraulic, pneumatic, thermal and electrical. The main design drivers of an aircraft are its range (weight and fuel consumption), its production and maintenance costs, and its environmental impacts [1]. Electrification of aircraft systems is a technological key to reach aircraft industry targets. Electrification is a process of penetration and propagation of electrical energy by reducing or substituting the use of other forms of energy, implementation of new and modernization of existing electrical devices [2–4].

Besides the aircraft network evolution, new methodologies must be developed in order to optimize in the same time each subsystem and the network operations. In a classical mechanistic design approach, the integrator defines several standards at the conceptual design phase (Fig. 1) in order to ensure a proper operating of the network when subsystems are connected. Even if subsystems are optimized by the electrical suppliers, the network is usually oversized [5,6].

Global approaches that integrate all components in a same optimization loop have shown good result on actuator systems [6,8,9]. The generalization of such approaches on a network containing a high number of subsystems provided by different suppliers faces the following questions:

*Corresponding author: Djamel Hadbi, University Grenoble Alpes, CNRS, G2Elab, F-38000 Grenoble, France. E-mail: Djamel.Hadbi@g2elab.grenoble-inp.fr.

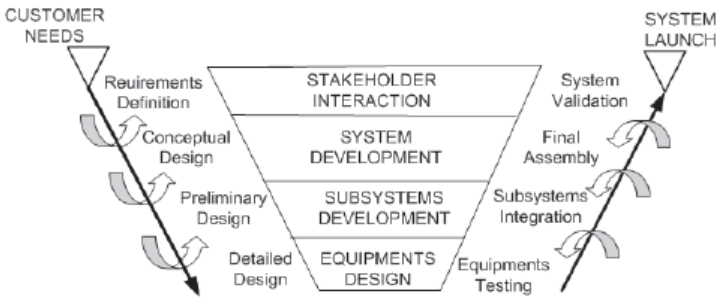

Fig. 1. The system design process [7].

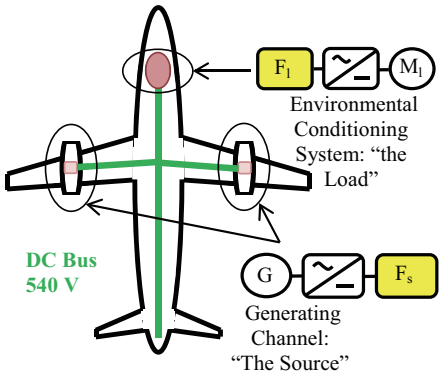

Fig. 2. General outline of the study case.

– Is it possible to gather in one model all system components while each component could be itself represented by a complex model? Is it relevant to use such models in a global optimization loop while ensuring convergence?
– On the other side, are subsystems suppliers willing to easily provide their models and their knowledge? Do they accept to transfer the design decision of their own equipment to the integrator?

In this paper, these issues are illustrated in a design problem of an aircraft network containing two electric subsystems: Subsystems are simplified and only the sizing of their filters is considered. The mechanistic approach based on the system decomposition is used firstly to show the current state of filter sizing. The global approach (industrially unachievable) is secondly applied to measure the possible mass gain.

Then, the Extended Pareto Front Method (EPFM) is presented. This method was initially introduced in [10] for the optimal design of an actuator devoted to an electrical vehicle. It is a collaborative approach based on a system decomposition that ensures the privacy of subsystem design.

2. Study case and specifications

A simplified case of 540 V HVDC (High Voltage Direct Current) network containing two subsystems is chosen to illustrate design strategies (Fig. 2). A 40 kW generating channel supplies a 40 kW environmental conditioning system used for air compression, the DC (direct current) current is 74 A. For methodological issues, a simplified representation with couplings is needed. Thus, we will restrict the electrical network description to the filters which are coupled through current and voltage harmonics. The issue here consists in designing the filter elements with minimum mass while fulfilling power quality constraints.

2.1. Model of the generating channel: Source modeling

In conventional aircraft networks, electrical energy is supplied by IDGs (Integrated Driven Generator). It is composed of 400 Hz synchronous machine that converts the hydromechanical power from the Engine Bleed Air system to HVDC network throw an ATRU (Auto TRansformer Unit) [10]. The ATRU generates high voltage DC (HVDC) source power using unregulated AC to DC power conversion with natural commutation operation and a voltage step down transformer. A capacitive output filter is used to reduce voltage harmonics before the connection to the 540 V HVDC bus.

Table 1
Rectifier current harmonics considered for the source

Characteristic frequencies (Hz)	$[I_{source}]_\omega$ (A)
2400	3.40
108 000	2.59 10^{-3}

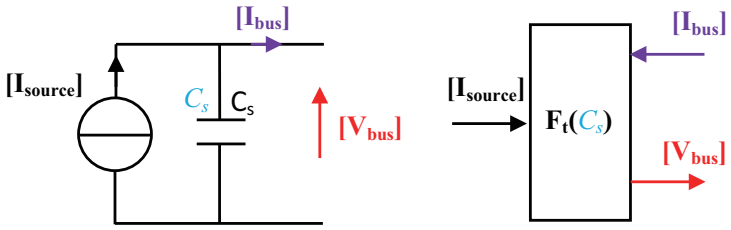

Fig. 3. Source filter model.

Current harmonics in the rectifier downstream have been identified for one operating point of the flight mission. Therefore, the part of the generating channel before the capacitive filter has been substituted by corresponding current sources (Fig. 3). Two main harmonics from (6 $k \times f_{\text{Generator}}$) spectrum are considered: 2400 Hz and 108 kHz (Table 1). This subsystem is referred as "source".

The "source" model is only represented by the bus capacity C_s. Source and bus currents are the input variables whereas the bus voltage is the output variable (Eq. (1)).

$$\left[\overrightarrow{\mathbf{V_{bus}}}\right]_\omega = \frac{\left[\overrightarrow{\mathbf{I_{source}}}\right]_\omega}{j \cdot C_s \cdot \omega} - \frac{\left[\overrightarrow{\mathbf{I_{bus}}}\right]_\omega}{j \cdot C_s \cdot \omega} \tag{1}$$

As the "source" is defined with characteristic frequencies, a matrix representation is used. Voltage and current variables are considered as vectors. Since source and bus current phases are not known, the worst case of phase shift is considered to calculate voltage harmonics (Eq. (2)).

$$\begin{cases} \left[\overrightarrow{\mathbf{V_{bus}}}\right]_\omega = SourceFt_{V_{bus}/I_{source}} \times \left[\overrightarrow{\mathbf{I_{source}}}\right]_\omega + SourceFt_{V_{bus}/I_{bus}} \times \left[\overrightarrow{\mathbf{I_{bus}}}\right]_\omega \\ SourceFt_{V_{bus}/I_{source}} = SourceFt_{V_{bus}/I_{bus}} = \dfrac{1}{C_s \cdot \omega} \end{cases} \tag{2}$$

A mass model is required to calculate the mass of the filter. Using datasheet from passive component manufacturer [11], a linear relation between the capacitance value and its mass can be obtained (Eq. (3)).

$$M_{Source}(kg) = 2666.67 \times C_s(\mu F) \tag{3}$$

2.2. *Model of the environmental conditioning system: Load modeling*

The environmental conditioning system is based on a High Speed Permanent Magnet Synchronous Machine (HSPMSM). This machine is controlled by an inverter. An input filter is used to extenuate the rejected harmonics on the DC bus.

Harmonic current components before filtering have been identified for the same operating point of the flight mission. Based on a PWM (Pulse-Width Modulation) control strategy, the inverter and the HSPMSM have been replaced with a current source delivering those harmonics (Fig. 4).

The characteristic frequencies depend on the switching frequency (here a $f_{swi} = 35$ kHz switching frequency is used to obtain the relevant current harmonics) and on the HSPMSM frequency ($f_{HSPMSM} = 1$ kHz) (Fig. 5) [12]. Two frequencies of high harmonic amplitudes are also included in the spectrum: 70 kHz ($2 \times f_{swi}$) and 140 kHz. ($4 \times f_{swi}$). An additional harmonic frequency common to the source at 108 kHz ($3 \times f_{swi} + 3 \times f_{HSPMSM}$) is finally considered to illustrate the case where the bus is polluted at the same time from both subsystems (Table 2). This subsystem is referred as "load".

Table 2

Inverter current harmonics considered for the load

Characteristic frequencies (Hz)	$[I_{load}]_\omega$ (A)
70 000	51.78
108 000	14.53
140 000	17.47

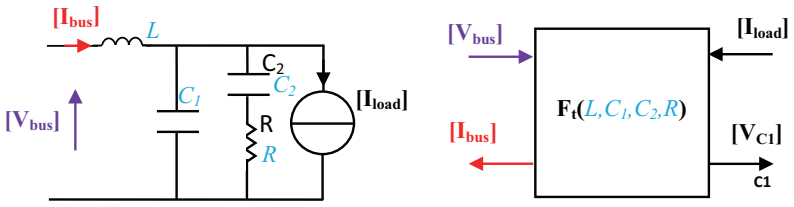

Fig. 4. Load filter model.

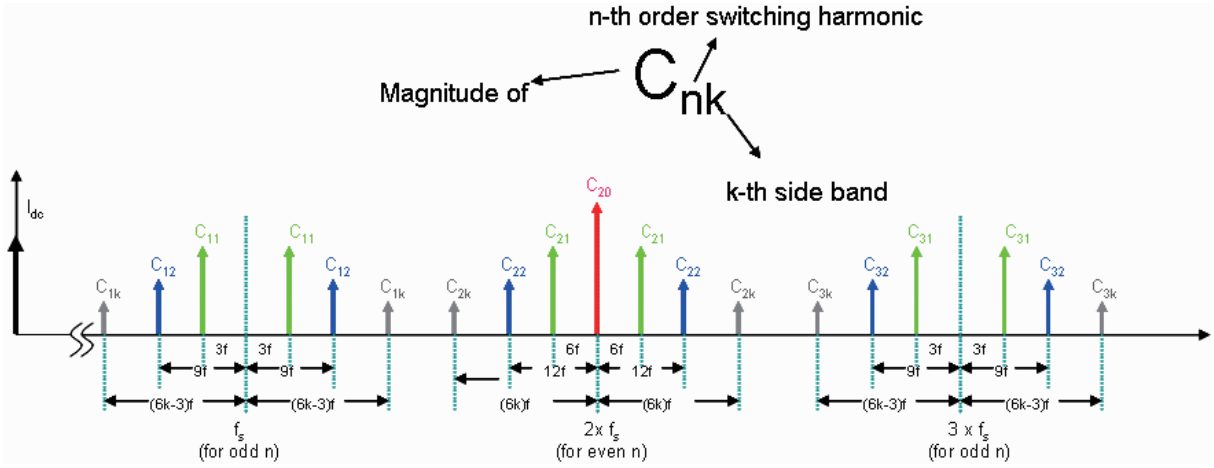

Fig. 5. Generic pattern of switching harmonics of DC link current idc [12].

The "load" model is only represented by its filter. The bus voltage and load current are the input variables and the bus current is the output variable of this subsystem (Eq. (4)).

$$\begin{bmatrix} \left[\overrightarrow{\mathbf{I_{bus}}}\right]_\omega \\ \left[\overrightarrow{\mathbf{V_{C_1}}}\right]_\omega \\ \left[\overrightarrow{\mathbf{V_{C_2}}}\right]_\omega \end{bmatrix} = \begin{bmatrix} j\cdot L\cdot\omega & 1 & 0 \\ 1 & -C_1\cdot\omega & -C2\cdot\omega \\ 0 & 1 & -(j\cdot R\cdot C_2\cdot\omega+1) \end{bmatrix}^{-1} \begin{bmatrix} \left[\overrightarrow{\mathbf{V_{bus}}}\right]_\omega \\ \left[\overrightarrow{\mathbf{I_{oload}}}\right]_\omega \\ \mathbf{0} \end{bmatrix} \tag{4}$$

Since load current and bus voltage phases are not known, we consider the worst case of phase shift to calculate the bus current harmonics (Eq. (5)).

$$\begin{cases} \left[\overrightarrow{\mathbf{I_{bus}}}\right]_\omega = LoadFt_{I_L/V_{bus}} \times \left[\overrightarrow{\mathbf{V_{bus}}}\right]_\omega + LoadFt_{I_L/I_{inv}} \times \left[\overrightarrow{\mathbf{I_{load}}}\right]_\omega \\ LoadFt_{I_{bus}/V_{bus}} = \left| \dfrac{-R\cdot C_1\cdot C_2\cdot\omega^2 + j(C_1+C_2)\omega}{1-(L\cdot C_1+L\cdot C_2)\cdot\omega^2 + j\cdot(R\cdot C_2\cdot\omega - L\cdot R\cdot C_1\cdot C_2\cdot\omega^3)} \right| \\ LoadFt_{I_{bus}/I_{load}} = \left| \dfrac{1+j\cdot R\cdot C_2\cdot\omega}{1-(L\cdot C_1+L\cdot C_2)\cdot\omega^2 + j\cdot(R\cdot C_2\cdot\omega - L\cdot R\cdot C_1\cdot C_2\cdot\omega^3)} \right| \end{cases} \tag{5}$$

The capacity sizing is similar to that presented for the source. It is used to design C_1 and C_2 too. The resistor mass is estimated by calculating its losses (Eqs (6) and (7)).

$$P_R = R\cdot I_R^2 \tag{6}$$

Table 3
Current Harmonics to be filtered

System characteristic frequencies (Hz)	$[I_{source}]_\omega$ (A)	$[I_{load}]_\omega$ (A)
2400	3.40	0
70 000	0	51.78
108 000	$2.59\ 10^{-3}$	14.53
140 000	0	17.47

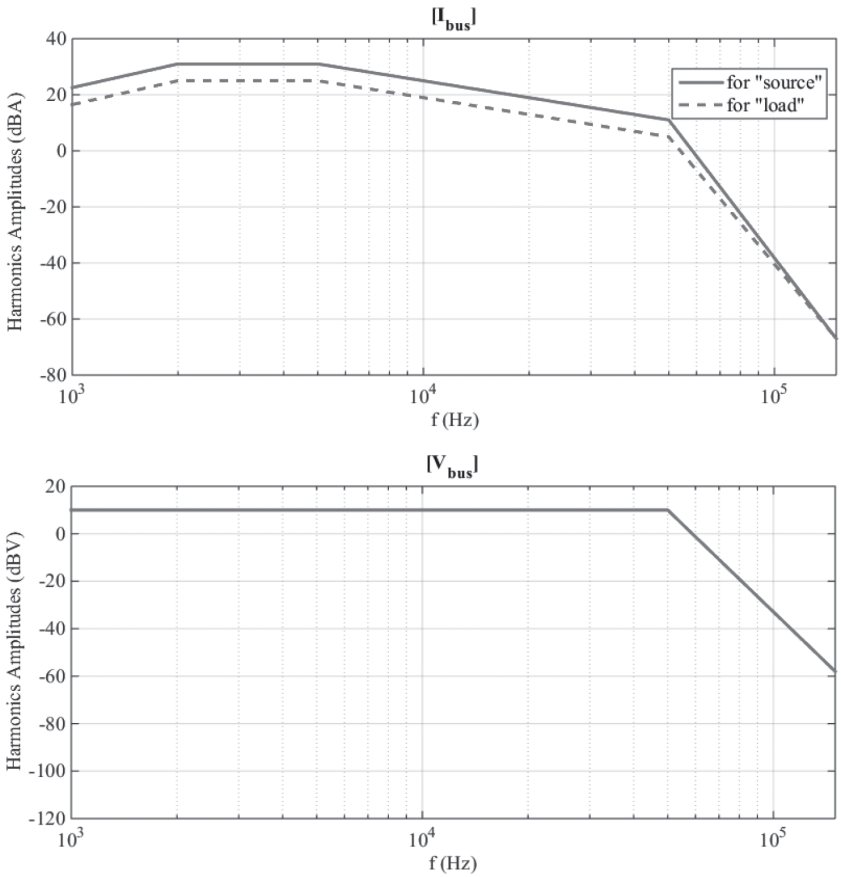

Fig. 6. Requirements on bus voltage and current ripple.

$$M_R = k_R \cdot P_R k_R = \frac{1}{2800}\ kg/W \tag{7}$$

The inductance mass is calculated using the geometric model presented in [13]. The load filter mass is the sum of passive elements masses (Eq. (8)).

$$M_{Load} = M_R + M_{C_1} + M_{C_2} + M_L \tag{8}$$

2.3. Design specifications

Both source and load must cooperate in safe and light weight operation. Light weight operation means that one objective which resides in the system weight minimization is considered (i.e. minimization of

Table 4
Harmonic limit of the 540 V DC bus

f	$[V_{bus}]^{STANDARD}$ (dBV)	$[I_{bus}]^{STANDARD}$ for "source"(dBA)	$[I_{bus}]^{STANDARD}$ for "load"(dBA)
2400 kHz	10.00	31.00	25.00
70 kHz	−11.13	−12.98	−17.05
108 kHz	−38.37	−43.68	−45.47
140 kHz	−54.67	−62.10	−62.48

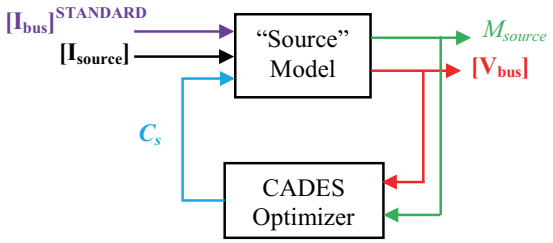

Fig. 7. Mechanistic design of the source filter.

the source + load filter masses). Safe operation means that source and load must fulfill voltage and current quality standards. Table 3 recalls source and load harmonics that must be filtered to obtain a clean HVDC bus.

In our example, harmonic standards on bus voltage and current are considered as constraints. Figure 6 shows an illustration of Airbus Directives standards [14]. The requirements for the HVDC voltage source are described with regard to a particular bus current: in steady-state conditions, the maximum differential-mode voltage ripple at the power terminals of the HVDC source shall be within the limits of Fig. 6-bottom when considering a current with a ripple within the envelope defined in Fig. 6-top. The spectral component amplitude is respectively given in dB from 1.0 VRMS and in dB from 1.0 ARMS.

Similarly, requirements for HVDC load currents are described with a particular bus voltage: In steady-state conditions, the differential-mode current ripple at HVDC load input shall be within the limits of Fig. 6-top when supplied with a steady-state voltage within the envelope defined in Fig. 6-bottom. Let us notice that current requirements for the source are higher than for the loads because the standards are planned for more than one load HVDC network. These standards are used in aircraft networks to ensure safe operations to all electric devices connected to the HVDC bus. Four main frequencies were chosen in the spectrum for the design problem. We summarize in Table 4 the values of standards for these particular frequencies.

3. Classical sizing of the filters

In a classical design approach called also "*mechanistic approach*", subsystems are separately designed. The system integrator (i.e. the aircraft manufacturer) only assembles the network components designed from quality standards by other suppliers.

3.1. Design of the source

3.1.1. Optimization problem formulation

The optimal design of the source is obtained by finding the value of its decision variable (here the bus capacity C_s) that minimizes the source weight while fulfilling quality standards (Fig. 6).

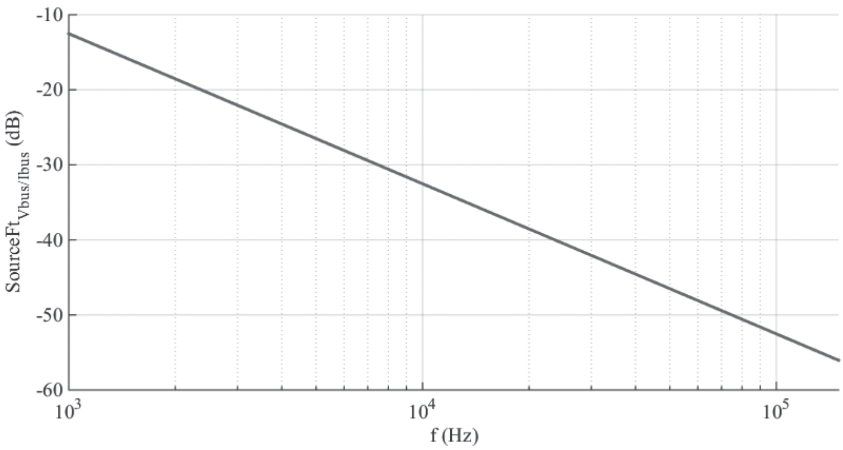

Fig. 8. Source transfer function shape.

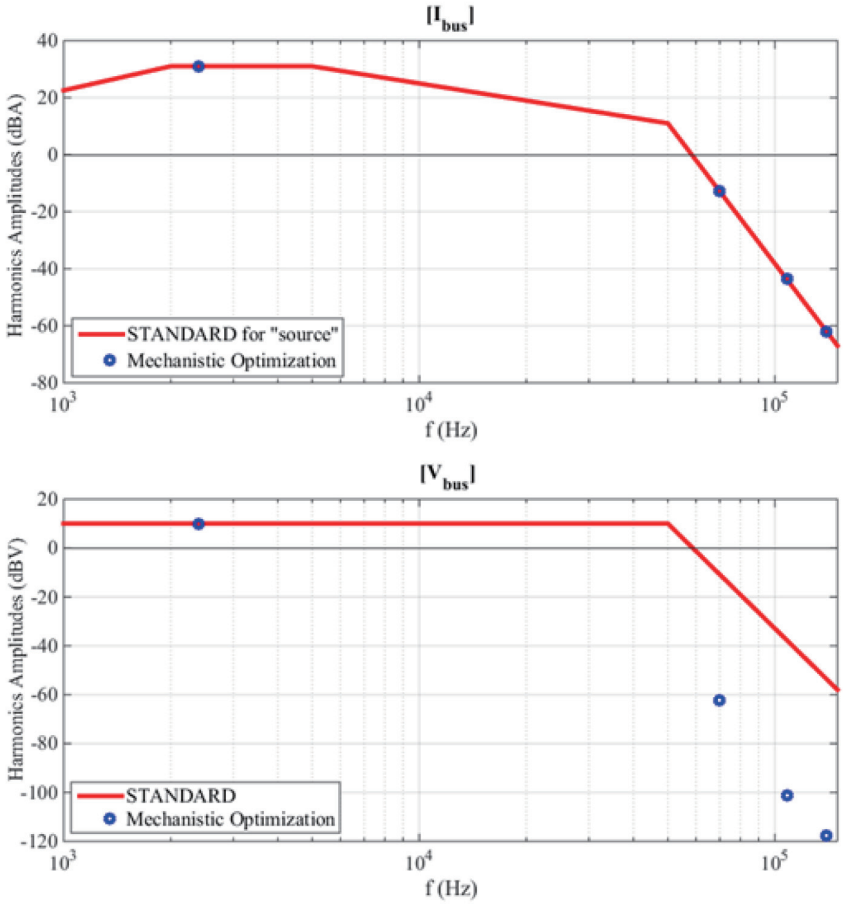

Fig. 9. Voltage and current harmonics in the mechanistic optimization of the source.

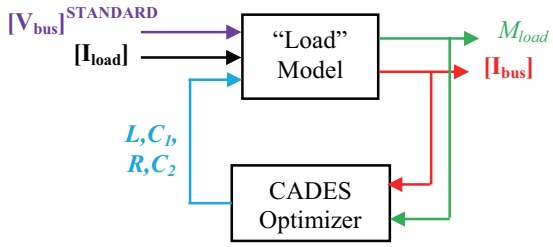

Fig. 10. Mechanistic design of the load filter.

In the source model, the bus current is an input variable. In the classical design approach, bus current harmonic values considered in the model are those of the worst case of quality standards (Fig. 7 and Eq. (9)) Voltage harmonics must remain under the maximal value permitted by the standards (Fig. 6-bottom).

The formulation of the optimization problem of the source in the classical approach is as follows:

$$\begin{cases} \min\limits_{C_s} \ W_{source} \\ \left[\overrightarrow{\|\mathbf{V_{bus}}\|}\right]_\omega \leqslant \left[\overrightarrow{\|\mathbf{V_{bus}}\|}\right]_\omega^{\mathbf{STANDARD}} \end{cases} \tag{9}$$

This optimization problem is solved using the SQP (Sequential Quadratic Programming) algorithm and the CADES package [15]. Mass and voltage are convex functions (Eqs (2), (3) and Fig. 8). Therefore, a deterministic algorithm can easily find the optimum.

3.1.2. Optimization results

The mass capacity obtained is 2.17 kg. The optimal design of the source is limited by the constraint of the first voltage harmonic at 2400 Hz. All other harmonic values are far under standards (Fig. 9).

3.2. Design of the load

3.2.1. Optimization problem formulation

The optimal design of the load is obtained by finding the values of its decision parameters (here the passive elements values C_1, C_2, L and R) that minimize the load weight while fulfilling quality standards (Fig. 10 and Eq. (10)).

In the load model, bus voltage is an input. In the classical design approach, bus voltage harmonic values considered in the model are those of the worst case of standards. Current harmonics must remain under the maximal value permitted by the standards.

The formulation of the optimization problem of the load in the classical approach is given in Eq. (10):

$$\begin{cases} \min\limits_{C_1,\, C_2,\, L,\, R} \ W_{\text{load}} \\ \left[\overrightarrow{\mathbf{I_{bus}}}\right]_\omega \leqslant \left[\overrightarrow{\mathbf{I_{bus}}}\right]_\omega^{\mathbf{STANDARD}} \end{cases} \tag{10}$$

The mass function (Eq. (8)) and the transfer function of the load (Eq. (5)) are convex functions in the range [1, 150] kHz (Fig. 11). Therefore, a deterministic optimization algorithm can be used.

The mass obtained is 2.24 kg and the design of the load is limited by the constraint of the last current harmonic at 140 kHz. The other harmonic values are under standards (Fig. 12).

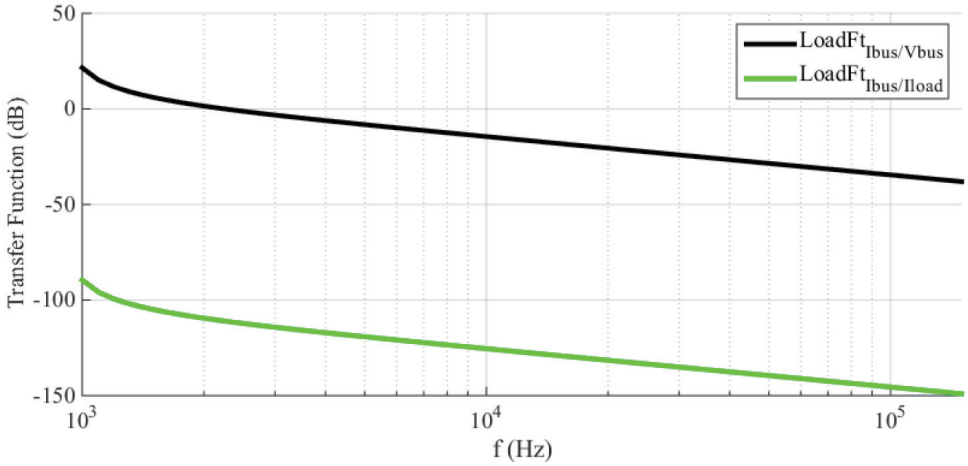

Fig. 11. Load transfer function shape.

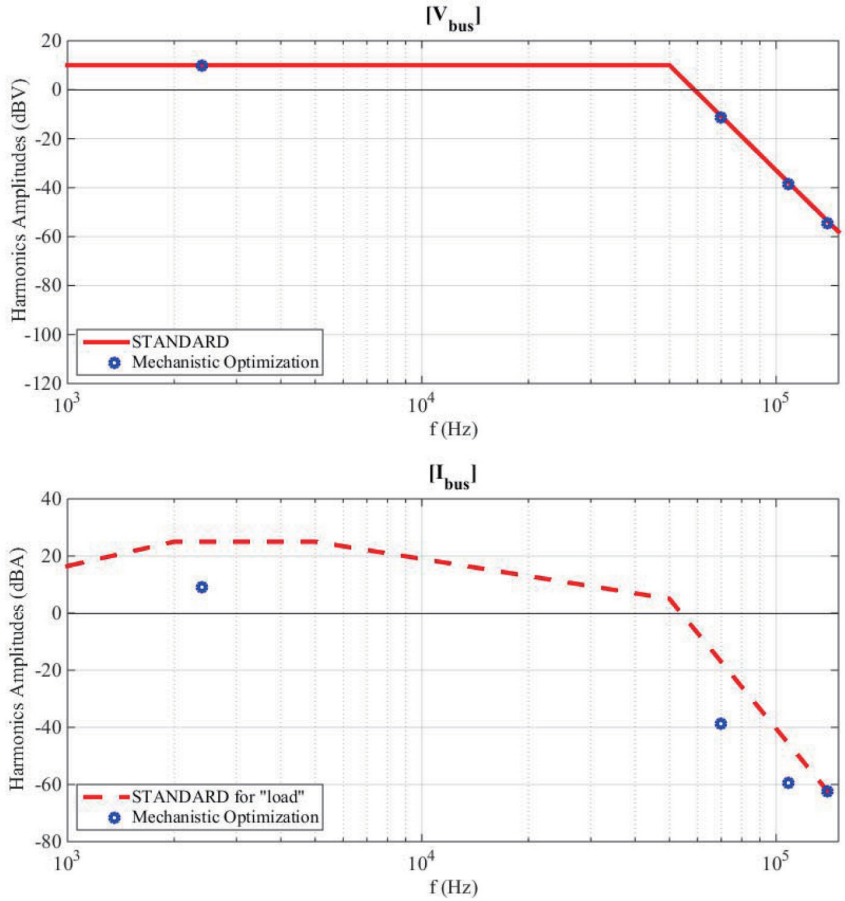

Fig. 12. Voltage and current harmonics in the mechanistic optimization of the load.

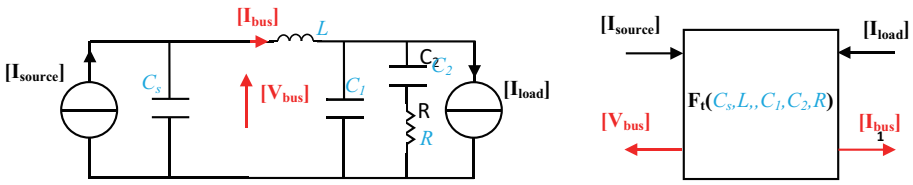

Fig. 13. Global system model.

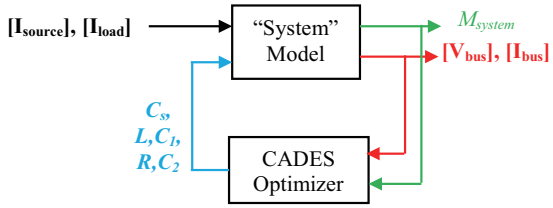

Fig. 14. Simultaneous design approach principle.

4. Simultaneous design approach

4.1. Optimization problem formulation

In the simultaneous design approach, the system is considered as a whole. The source and the load are described in the same system model (Eq. (11)).

$$\begin{bmatrix} \left[\overrightarrow{\mathbf{I_{bus}}}\right]_\omega \\ \left[\overrightarrow{\mathbf{V_{bus}}}\right]_\omega \\ \left[\overrightarrow{\mathbf{V_{C_1}}}\right]_\omega \\ \left[\overrightarrow{\mathbf{V_{C_2}}}\right]_\omega \end{bmatrix} = \begin{bmatrix} j\cdot L\cdot\omega & -1 & 1 & 0 \\ 1 & j\cdot C_s\cdot\omega & 0 & 0 \\ 1 & 0 & -j\cdot C_1\cdot\omega & -j\cdot C_2\cdot\omega \\ 0 & 0 & 1 & -(1+j\cdot R\cdot C_2\cdot\omega) \end{bmatrix}^{-1} \begin{bmatrix} 0 \\ \left[\overrightarrow{\mathbf{I_{source}}}\right]_\omega \\ \left[\overrightarrow{\mathbf{I_{load}}}\right]_\omega \\ 0 \end{bmatrix} \tag{11}$$

Both bus voltage and current are now calculated in the model. Input variables are the source current and the load current harmonics only. There is no worst case assumption on the bus voltage and current values (Fig. 13).

The optimal design of the system is obtained by finding the values of all decision variables that minimize the sum of source and load weights while fulfilling both voltage and current harmonic constraints (Fig. 14).

Equation (12) gives the optimization problem formulation with the simultaneous design approach:

$$\begin{cases} \min\limits_{C_s, C_1, C_2, L, R} W_{System} \\ \left[\overrightarrow{\mathbf{V_{bus}}}\right]_\omega \leqslant \left[\overrightarrow{\mathbf{V_{bus}}}\right]_\omega^{\mathbf{STANDARD}} \\ \left[\overrightarrow{\mathbf{I_{bus}}}\right]_\omega \leqslant \left[\overrightarrow{\mathbf{I_{bus}}}\right]_\omega^{\mathbf{STANDARD}} \end{cases} \tag{12}$$

The optimization problem in the simultaneous design approach may be non-convex because the transfer functions (Eqs (13) and (14)) are multimodal (Fig. 15). As a consequence, deterministic optimization

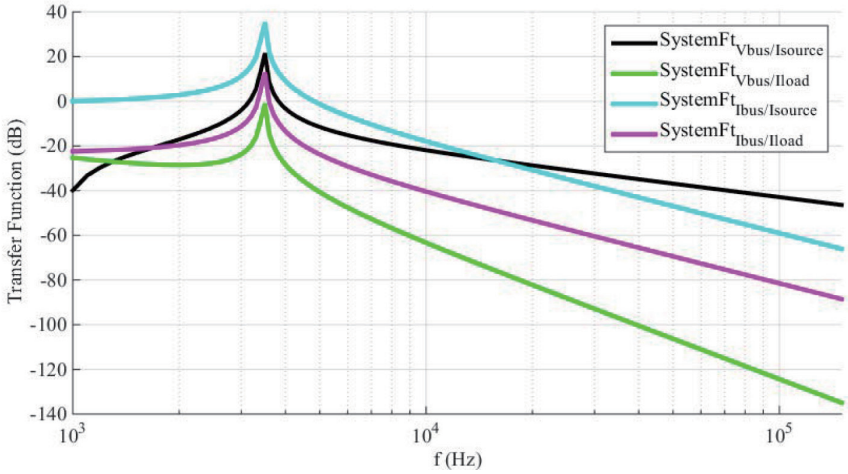

Fig. 15. System transfer functions.

algorithm could be trapped in a local optimum. To avoid this problem, 10 random initializations of the SQP algorithm are used to find the global optimum.

$$\begin{cases} V_{bus_f} = SystemFt_{V_{bus}/I_{source}}(C_s, L, C_1, C_2, R) \times I_{source_f} \\ \qquad +SystemFt_{V_{bus}/I_{load}}(C_s, L, C_1, C_2, R) \times I_{load} \\ SystemFt_{V_{bus}/I_{source}} = \dfrac{1 - L \cdot (C_1 + C_2)\,\omega^2 - j\left(L \cdot C_1 \cdot C_2 \cdot R \cdot \omega^3 - C_2 \cdot R \cdot \omega\right)}{D} \\ SystemFt_{V_{bus}/I_{load}} = \dfrac{-1 - j \cdot C_2 \cdot R \cdot \omega}{D} \\ D = C_s \cdot L \cdot C_1 \cdot C_2 \cdot R \cdot \omega^4 - C_2 \cdot R\,(C_s + C_1)\,\omega^2 \\ \qquad -j\left(C_s \cdot L\,(C_1 + C_2)\,\omega^3 - (C_s + C_1 + C_2)\,\omega\right) \end{cases} \tag{13}$$

$$\begin{cases} I_{bus_f} = SystemFt_{I_{bus}/I_{source}}(C_s, L, C_1, C_2, R) \times I_{source_f} \\ \qquad +SystemFt_{I_{bus}/I_{load}}(C_s, L, C_1, C_2, R) \times I_{load} \\ SystemFt_{I_{bus}/I_{source}} = \dfrac{-C_1 \cdot C_2 \cdot R \cdot \omega^2 + j\,(C_1 + C_2)\,\omega}{D} \\ SystemFt_{I_{bus}/I_{load}} = \dfrac{-C_s \cdot C_2 \cdot R \cdot \omega^2 + j \cdot C_s \cdot \omega}{D} \end{cases} \tag{14}$$

4.2. Optimization results

The total mass obtained is 2.56 kg. The system design is limited by the constraint of the last current harmonic at 140 kHz and the constraint of the first voltage harmonic at 2400 Hz (Fig. 16).

4.3. Why the optimal solution of the simultaneous design approach is better?

The total mass of the system in the mechanistic design approach is 4.41 kg (2.17 + 2.24) while it equals 2.56 kg in the simultaneous design approach (Table 5).

A difference of 42% is due to the local view in the mechanistic design approach. Indeed, in this approach, either bus current (in the design of the source) or voltage bus (in the design of the load)

Table 5
Optimal solution comparisons

	Mechanistic design approach	Simultaneous design approach
M_{source} (kg)	2.17	0.35
M_{load} (kg)	2.24	2.21
M_{system} (kg)	4.41	2.56

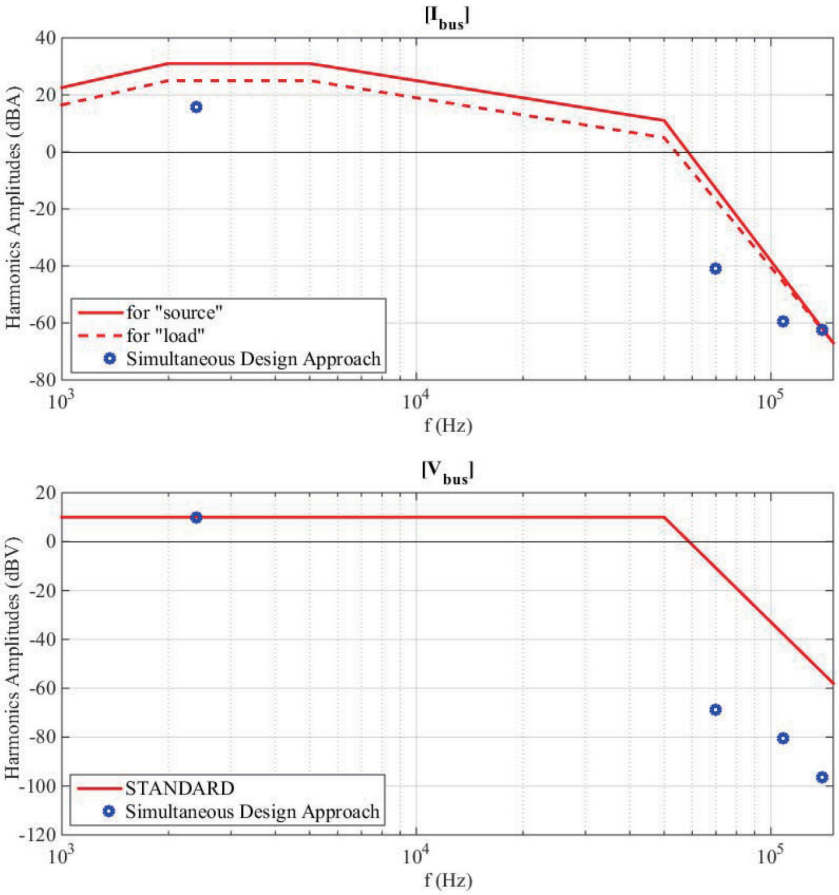

Fig. 16. Simultaneous design approach results.

are considered as standards limit values (Figs 9 and 12). This leads to the oversizing of both filters. Conversely, in the simultaneous design approach, the real values of voltage and bus current are calculated depending on all network variables.

5. Extended Pareto Front Method (EPFM)

In the previous section, it has been shown that the simultaneous design approach succeeds in reaching the best design because it gets the optimal values of the harmonic components. Let us remember that the simultaneous design approach is industrially no achievable because it requires sharing the models and the design variables. EPFM is a decomposed based approach. There are several approaches based

Table 6
Matrix of dependencies [19] related to the studied system

		Decision variables			
Objectives	M_{source}	C_s	0	0	0
	M_{load}	0	C_1	C_2	L
Coupling variables	$[V_{bus}]$	C_s	C_1	C_2	L
	$[I_{bus}]$	C_s	C_1	C_2	L

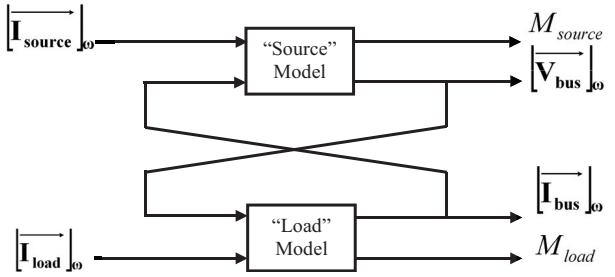

Fig. 17. Couplings building in EPFM.

on hierarchical decomposition, some of them have been developed in MDO (Multidisciplinary Design Optimization) context [16–18]. EPFM is different because there is no system optimizer at the integrator level.

EPFM aims at reaching the optimal system design without sharing the models. In the considered case of filter design, it consists in identifying the same bus current and voltage values as in the simultaneous design approach (Fig. 16). A collaborative process exploiting those variables to meet the system optimal design is needed. Such variables are qualified as coupling variables [10] (Fig. 17).

In the HVDC studied network, bus voltage and current are the coupling variables represented by their frequency harmonics. Their values depend on all decision variables (C_s, C_1, C_2, L and R). Instead of looking for the optimal values of the decision variables, we try to find the corresponding values of the coupling variables (Eq. (15)).

$$\begin{cases} \left[\overrightarrow{\mathbf{V_{bus}}}\right]_\omega^{\mathbf{source}} = \left[\overrightarrow{\mathbf{V_{bus}}}\right]_\omega^{\mathbf{load}} = \left[\overrightarrow{\mathbf{V_{bus}}}\right]_\omega^{\mathbf{system}} \\ \left[\overrightarrow{\mathbf{I_{bus}}}\right]_\omega^{\mathbf{source}} = \left[\overrightarrow{\mathbf{I_{bus}}}\right]_\omega^{\mathbf{load}} = \left[\overrightarrow{\mathbf{I_{bus}}}\right]_\omega^{\mathbf{system}} \end{cases} \tag{15}$$

5.1. Assumptions related to this approach

The following condition should be met for designing a system with N components: The system objective function should be computed from the corresponding objective functions of its subsystems (Eq. (16)). In our case, $N = 2$ which means:

$$M_{system} = M_{source} + M_{load} \tag{16}$$

5.2. Analysis of component couplings in a system

There are many ways to describe the couplings in a system. The matrix of dependencies is a one of analysis methods that describes the couplings between functions and variables [19].

The direct dependencies between decision variables and other variables depend on the physic modeling of the system. Source and load masses are depending on their decision variables only. On the other hand, voltage and current bus depend on all decision variables. Thus, the coupling between source and load masses is indirect through electric variables of the bus (Table 6).

Coupling variables can be inputs or outputs according to the subsystem design. In EPFM, only coupling input variables are considered because the output coupling variables are resulting from the sizing optimization. Considering 4 characteristic frequencies (Table 3) $N_f = 4$ harmonic variables are used to represent the coupling variables in order to ensure the consistency at the integrator (system) level. Those coupling variables are discretized with a uniform sampling of N_s points in the range defined by the standards.

Table 7
EPFM results with different sampling of the coupling variables

N_s	3	4	5	6	7	8
Γ_{source} or Γ_{load}	81	256	626	1296	2401	4096
Γ_{comp}	6 561	65 536	390 625	1 679 616	5 764 801	16 777 216
N_{sys}	92	967	5 023	19 054	47 239	114 822
$\frac{N_{sys}}{\Gamma_{comp}}(\%)$	1.40	1.48	1.29	1.13	0.82	0.68
M_{system}	3.41	3.07	2.91	2.80	2.74	2.69

5.3. Source space solution

A mechanistic optimization design of the source calculates the optimal value of the source mass from overestimated harmonic currents. In the EPFM, the current bus values are not fixed by the standards but sampled in a range with N_s points. It should be noted that this number of sampling points per coupling variables could be different. The resulting source solution space is defined as the total number of discrete combinations of the coupling variables (Γ_{source}) according to Eq. (17).

$$\Gamma_{source} = N_s^{N_f} \tag{17}$$

For each combination in the source solution space, an optimization consisting in minimizing the source filter weight is performed with the corresponding values of the bus current harmonics.

5.4. Load space solution

The load solution space is built using the same method as the source solution space. Given a number of sampling points N_s, all bus voltage configurations are used to perform Γ_{load} independent optimizations (Eq. (18)).

$$\Gamma_{load} = N_s^{N_f} \tag{18}$$

In our case, the load and source solution spaces have the same size.

5.5. Consistency test and calculation of the system solution

Given both source and load solution spaces, each solution from the source space is compared to all solutions of the load space. The number of comparisons N_{comp} is defined by Eq. (19).

$$\Gamma_{comp} = \Gamma_{source} \times \Gamma_{load} \tag{19}$$

The aim of this comparison step is to identify the consistent solutions that fulfill Eq. (15) with 1% of tolerance, ensuring the consistency of the coupling variable constraints. For those solutions, the total mass is calculated by adding the source and load filter masses. The number of consistent solutions identified is denoted as N_{syst}. Among those consistent solutions, the optimal system solution is that with the smallest mass M_{system}.

5.6. Optimization results

Table 7 gives the EPFM results for number of sampling points N_s. When N_s increases, the solution space becomes larger. In the same time more comparisons are required to find the consistent solutions. The smaller the discretization, the better the accuracy achieved on the optimal system solution. However it should be noted that EPFM with the less accurate sampling ($N_s = 3$) provides a better solution than the mechanistic approach (23% of mass gain). Finally, the rate between consistent solutions and all comparisons performed between the source and load solutions decreases with the increase of N_s.

6. Comparison between all approaches

6.1. Computational cost

The system mass obtained using the three approaches has already been given in the previous sections. Let us focus on now on time computation. All CPU time presented in the following have been obtained under the same conditions with the same computer.[1] In the mechanistic approach, subsystem optimizations could be done in parallel. Therefore, the CPU time required for obtaining the mechanistic solution is imposed by the highest CPU time between the source and load optimizations. The load filter is more complex than the source, so its CPU time is higher ($T_{mecha.load} = 183$ ms versus $T_{mecha.source} = 43$ ms). Similarly, due to a higher level of coupling in the global system model, the CPU time of the simultaneous design approach ($T_{simultaneous} = 399$ ms) is higher than the cumulative CPU time of both designs in the mechanistic approach. The EPFM CPU time is the sum of the time (T_{opti}) required for generating the solution space from the independent optimizations and the CPU time (T_{comp}) dedicated to the solution comparisons for identifying the consistent configurations and the optimal solution (Eq. (20)).

$$T_{EPFM} = T_{opti} + T_{comp} \tag{20}$$

For N_s different values, T_{opti} and T_{comp} are given in Fig. 18(a). Figure 18(b) displays the total CPU time of EPFM (T_{EPFM}). When using $N_s = 8$ the best EPFM system mass is obtained (2.69 kg) with a computational cost of 6282 s (almost two hours).

What about a more complex system with more loads and more harmonic frequencies for better accuracy?

If a case study with more than one load is considered, the EPFM CPU time will not necessarily increase since all load optimizations can be performed in parallel: T_{opti} will typically depend on the slowest load optimization. The consistency condition will change as the bus current will be defined as the sum of all load currents (Eq. (21)). However, the number of comparisons, only depending on two equality constraints on the bus current and voltage, will be the same as for one single load.

$$\begin{cases} \left[\overrightarrow{\mathbf{V_{bus}}}\right]_{\omega}^{\mathbf{source}} = \left[\overrightarrow{\mathbf{V_{bus}}}\right]_{\omega}^{\mathbf{load}} = \left[\overrightarrow{\mathbf{V_{bus}}}\right]_{\omega}^{\mathbf{system}} \\ \left[\overrightarrow{\mathbf{I_{bus}}}\right]_{\omega}^{\mathbf{source}} = \sum_{N_{loads}} \left[\overrightarrow{\mathbf{I_L}}\right]_{\omega}^{\mathbf{load}} = \left[\overrightarrow{\mathbf{I_{bus}}}\right]_{\omega}^{\mathbf{system}} \end{cases} \tag{21}$$

Conversely, considering more harmonic frequency will increase the CPU time due to the increase of the number of comparisons required for identifying all consistent solutions.

6.2. Collaboration level

Regarding the information shared and needed in each approach three collaboration levels can be identified (Table 8). The highest collaboration level is for the simultaneous design approach where it is required to share all subsystems modeling to build a single optimization loop at the system level. EPFM presents an intermediate level of collaboration providing more than one solution through a set of optimizations guided by the standards and the coupling variables at the system level. Finally, the classical mechanistic approach presents the smaller level of collaboration only sharing the HVDC standards.

[1] Intel® Core(TM) i5-3317U CPU @ 1.70 GHz, avec 6 GB de RAM, sur Windows 8.1 64-bit.

Table 8
Comparison of the different design approaches

Approach	System mass (kg)	Time calculation (s)	Collaboration level
Mechanistic approach	4.41	0.183	Standards
EPFM	2.69	6282	Standards + solution spaces
Simultaneous design approach	2.56	0.399	Standards + modeling

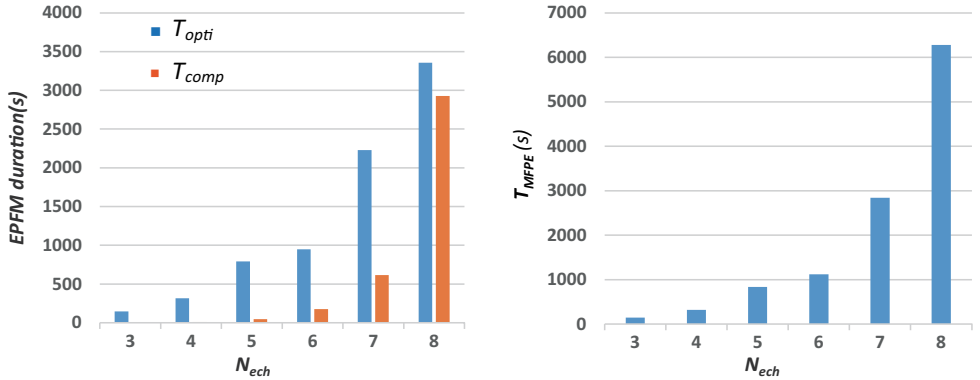

Fig. 18. EPFM time calculation.

As presented in Table 8, using the EPFM allows finding a system mass close to the best mass obtained with the simultaneous design approach. Compared with the mechanistic design, there is 39% of mass gain with $N_s = 8$. The CPU time calculation is quite high for this simple study case. Regarding collaboration level, it would be acceptable for electric equipment suppliers to give more than one design. Once their design problems are built, they could easily change input values to obtain more than one solution. Even if their time calculations are high, solutions exist to accelerate optimization process by using parallel computing.

7. Conclusion

In this work, three different design approaches have been applied for the sizing of electric filters of a typical aircraft network. Through this simple study case, advantages and drawbacks of each approach have been discussed with regard to multiple criteria: system optimality (here the filter mass reduction), CPU time and level of collaboration. It has been shown that the EPFM can constitute a good compromise between those criteria in comparison with conventional design approaches such as mechanistic or simultaneous designs. The main drawback of the EPFM resides in the increase of the CPU time with the increase of the number of coupling variables and their associated sampling. However, some improvements of the EPFM could probably be done by exploiting combinatorial optimization for a quicker identification of the consistent solutions.

References

[1] S. Liscouet-Hanke and K. Huynh, A Methodology for Systems Integration in Aircraft Conceptual Design – Estimation of Required Space, No. 2013-01-2235, SAE 2013, 1–5.

[2] A. Fraj, M. Budinger, T. El Halabi, J.C. Maré and G.C. Negoita, Modelling approachs for the simulation-based preliminary design and optimization of electromechanical and hydraulic actuations systems, In: *53rd AIAA/ASME/ASCE/AHS/ ASC Structures, Structural Dynamics and Materials Conference 20th AIAA/ASME/AHS Adaptive Structures Conference 14th AIAA*, 2012, pp. 1523–1538.
[3] S. Chiesa, Methodology for an Integrated Definition of a System and Its Subsystems: The Case-Study of an Airplane and Its Subsystems, Edited by InTech in Systems Engineering-Practice and Theory, 2012. ISBN 978-953-51-0322-6.
[4] C. Avery, S. Burrow and P. Mellor, Electrical generation and distribution for the more electric aircraft, in: *Univ. Power. Eng. Conf.*, 2007, pp. 1007–1012.
[5] X. Roboam, B. Sareni and A. De Andrade, More Electricity in the Air: Toward Optimized Electrical Networks Embedded in More Electrical Aircraft, Industrial Electronics Magazine, IEEE Volume: 6, Dec. 2012, 6–17.
[6] Airbus and United Technologies, Final report joint UTC/Airbus ITAPS study, Technical report, May 2005.
[7] X. Giraud, M. Sartor, X. Roboam, B. Sareni, H. Piquet, M. Budinger and S. Vial, Load allocation problem for optimal design of aircraft electrical power system, *International Journal of Applied Electromagnetics and Mechanics* **43** (n° 1-2) (2014), 1–13. ISSN 1383-5416.
[8] D. Hadbi, N. Retière, F. Wurtz, X. Roboam and B. Sareni, Comparison between system design optimization strategies for more electric aircraft, 13th International Workshop on Optimization and Inverse Problems in Electromagnetism, Sep 2014, Delft, Netherlands, 51–52,
[9] X. Roboam, Integrated design by optimization of electrical energy systems, edited by ISTE Wiley, 320 pages, 2012. ISBN 978-1-84821-389-0.
[10] H. Nguyen-Huu, N. Retière and F. Wurtz, Optimization of an electrical system using Pareto borders of each component, Application to an automotive drive chain, IEEE Industrial Electronics, IECON 2006, 2006, 3662–3667.
[11] www.avx.com/, Manufacturer and supplier of electronic components.
[12] H. Zhang and Q. Zhao, Switching Harmonics in a Three-Phase PWM Inverter, SAE Technical Paper 2006-01-3078, 2006, doi: 10.4271/2006-01-3078.
[13] F. Leplus, Bobine à noyau de fer en régime variable, Techniques de l'ingénieur D-3040, 2007, 1–5.
[14] Airbus Directives (ABD) and Procedures, ABD0100-Equipment-Design, General Requirements For Suppliers. Issue C, 1998, 1–71.
[15] Vesta-System, Cades Solutions, http://www.cades-solutions.com/cades/.
[16] J.S. Sobieski, B. James and A.R. Dovi, Structural optimization by multilevel decomposition, *Am. Inst. Aeronaut. Astronaut.* **21** (1985), 1291–1299.
[17] S. Tosserams, A.T. Hofkamp, L.F.P. Etman and J.E. Rooda, A specification language for problem partitioning in decomposition-based design optimization, *Struct. Multidiscip. Optim.* **42** (2010), 707–723.
[18] A.C. Berbecea, Multi-level approaches for optimal system design in railway applications (Ph.D. dissertation), Université des sciences et technologie de Lille, 2012.
[19] J.-F.M. Barthelemy, Engineering design application of multilevel optimization methods, in Computer Aided Optimum Design of Structures, Brebbia, CA, S. Hernandez, ed. Berlin, Germany: Springer-Verlag, 1989, 113–122.